Supporting Information

Warden et al. 10.1073/pnas.1321605111

SI Methods

Participants. One hundred three throwing athletes and 94 aged-matched controls were recruited. Throwers were recruited into three groups: (*i*) active ($n = 9$), (*ii*) former ($n = 84$), and (*iii*) continuing ($n = 10$) throwers. Active throwers were recruited to explore the location and magnitude of skeletal adaptation within the humerus associated with overhand throwing and were included if they were currently competing as a pitcher in Major (MLB) or Triple-A level Minor (MiLB) League Baseball. Former throwers were recruited at different time periods after the end of their professional careers to explore the lifelong maintenance of the skeletal benefits conferred by elevated mechanical loading during youth. They were included if they (*i*) had played in at least one game of MLB as a pitcher or catcher during their professional career and (*ii*) had not participated in any baseball games or participated more than three times per year in any throwing activity since leaving professional baseball. Pitchers and catchers were included because college-level players at these positions previously have been shown to have equivalent side-to-side differences in humeral bone properties (1). Former throwers were divided into decades of years detraining (i.e., the number of years since they stopped throwing) for analyses. Continuing throwers were recruited to explore the benefit of mechanical loading continued into later adulthood and were included if they (*i*) had played in at least one game of MLB as a pitcher during their professional career, (*ii*) were aged 65–80 y, and (*iii*) threw a minimum of three times per week for at least 20 y after the cessation of their professional baseball career.

Throwers and controls were excluded if they reported a history of (*i*) disease known to influence skeletal metabolism; (*ii*) taking pharmacological agents known to influence skeletal metabolism; (*iii*) humeral fracture or stress fracture; (*iv*) fracture or stress fracture of any other upper extremity bone within the past 2 y; or (*v*) participating more than once per month for longer than 6 mo in an athletic activity [including racquet sports, volleyball, football (at the quarterback position), discus throw, javelin, shot-put, and bowling] or vocation (such as general contracting or other manual labor) that primarily involved unilateral use of an upper extremity (other than baseball in throwers). Active throwers were recruited from a local Triple A-level MiLB baseball team. Former and continuing throwers were recruited from the contiguous United States via self-referral after distribution of study flyers. Controls were recruited from the local Indianapolis region. All assessments were performed in Indianapolis, IN, except for the assessment of throwing biomechanics in a MLB player, which was performed in Birmingham, AL. Study procedures were approved by the Institutional Review Boards at Indiana University and St. Vincent's Birmingham, and all subjects provided written informed consent before participation.

Strain Within the Humerus During Throwing. Muscle and glenohumeral joint forces at the time of maximal joint torques during a fastball pitch performed by a professional MLB player were calculated using a musculoskeletal model developed from high-resolution CT images of the bones and color cryosection images of the arm muscles obtained from the Visible Human Male dataset (2). The calculated loads were applied to a finite element (FE) model of the humerus of the professional MLB/MiLB player to calculate diaphyseal tensile and shear strains (Fig. S1).

Thirteen degrees of freedom described the positions and orientations of seven bones (clavicle, scapula, humerus, radius, ulna, carpal bones, and the hand) in the musculoskeletal model. The model was actuated by 42 muscle subregions, which represented the actions of 26 muscle groups in the upper limb. Each muscle–tendon actuator was represented as a three-element muscle in series with tendon. The inertial properties and muscle–tendon parameters assumed in the model were based on data published by Garner and Pandy (3). The path of each muscle was calculated using a computational algorithm based on the obstacle-set method (4). The modeled muscle paths were validated by quantitatively comparing moment arms calculated in the model against measurements obtained from cadaver specimens (2).

3D MR images (Magnetom Verio; Siemens Medical Solutions) of muscles attaching to the arm were obtained from the professional MLB/MiLB player using a Dixon volumetric interpolated breath-hold examination T1-weighted sequence with the following parameters: repetition time/echo time 7.14/3.68 ms, slice thickness 4 mm, field of view 337 × 399 mm, matrix 292 × 384 pixels, bandwidth 123 Hz, and flip angle 20°. The resulting voxel size was $1.04 \times 1.04 \times 4$ mm^3. All 42 muscle subregions in the model were segmented using image-processing software (Amira, Visualization Sciences Group), and the volume of each muscle was calculated directly from the MR images. 3D joint angles at the shoulder and elbow during a fastball pitch by the professional MLB/MiLB player were measured at the American Sports Medicine Institute (Birmingham, AL), and inverse dynamics was used to calculate the corresponding net joint torques, as previously described (5). The net joint torques were decomposed into individual muscle forces by minimizing the sum of the squares of all muscle stresses subject to the physiological bounds imposed by each muscle's force-length-velocity properties (3, 6).

The muscle forces and joint reaction forces then were applied to an FE model of the humerus of the professional MLB/MiLB player. The geometry of the player's humerus was segmented from CT data (obtained as described below in *Quantitative Computed Tomography*) and was converted into 3D solid models (Geomagic v10; Geomagic). Each element within the FE mesh (quadratic tetrahedral, average length = 3.1 mm) was assigned a Young's modulus based on the X-ray attenuation values (in Hounsfield units) and apparent density using calibration functions derived from a five-material CT phantom (Mindways Software, Inc.) placed below the subject at the time of scanning (7).

The muscle and joint reaction forces were applied to the FE model as nodal point loads. The muscle insertion sites were scaled to the geometry of the humerus and were adjusted to lie on the bone surface. The location of the glenohumeral joint reaction force was calculated as the intersection of the joint reaction force vector passing through the center of the humeral head. A series of nodes at the center of the olecranon of the distal humerus were kinematically constrained to model the reaction force at the elbow joint. Three nodes on the medial and lateral aspects of the distal humerus were constrained to model ligament forces. A single node at the glenohumeral joint center was used to affix linear spring elements to model the passive soft tissue restraint. A linear stress analysis was used to calculate the maximum principal strain and von Mises stress at each node using Abaqus v11.1 (Dassault Systèmes). Results from elements within a 4-mm radius of the nodal boundary conditions were ignored to avoid errors resulting from boundary effects.

Shoulder Muscle Strength and Range of Motion. Bilateral concentric shoulder external and internal rotation torques and the bilateral range of shoulder internal and external rotation were assessed in former and continuing throwers and their controls, as previously

described (1). Shoulder muscle strength and range of motion were not assessed in active throwers, because study visits were performed on player rest days during the baseball season.

Dual-Energy X-Ray Absorptiometry. Dual-energy X-ray absorptiometry (DXA) (Discovery-W; Hologic, Inc.) was used to obtain whole-body (minus the head), hip, and lumbar spine areal bone mineral density (g/cm^2). Whole-body scans also provided measures of whole-body lean mass (kg), percent fat mass (%), whole-arm bone mineral content (g), and areal bone mineral density (g/cm^2) and lean mass (kg).

Quantitative CT. The bilateral humerii of active throwers and their controls were imaged using a multislice helical CT scanner (Phillips Brilliance 64; Philips Medical Systems) operating at 120 kV peak, 400 mA, 64 × 0.625 collimation, and pitch 0.6. Scan volumes included the entire humerus and included phantoms containing calcium hydroxyapatite standards embedded in water-equivalent resin. Images were axially reconstructed with a 1.0-mm slice width spaced 0.5 mm apart using a 768 × 768 matrix and field of view of <30 cm (reconstructed voxel size $<0.39 \times 0.39 \times 1.0$ mm^3). Tomographic images at 5% increments of humeral length were imported into ImageJ v1.45s (National Institutes of Health) for analysis using customized macros. The outer bone edge was segmented with a threshold of 700 mg/cm^3; a threshold of 300 mg/cm^3 was used to separate the cortical and subcortical/trabecular bone compartments. Parameters obtained were cortical volumetric bone mineral density (mg/cm^3), cortical bone mineral content (mg/mm), total area (cm^2), cortical area (cm^2), medullary area (cm^2), average cortical thickness (mm), polar moment of inertia (cm^4), and the minimum and maximum second moments of area (cm^4). The linear relationship between Hounsfield units and known densities of the calcium hydroxyapatite standards was exploited to determine voxel density (mg/cm^3).

In all throwers (active, former, and continuing) and controls the midshaft humerus in both upper extremities was assessed by peripheral quantitative CT (pQCT) (XCT 3000; Stratec Medizintechnik GmbH), as previously described (1). pQCT was performed at the midshaft humerus in the detraining studies, rather than at the location of greatest adaptation observed from the QCT assessments in active throwers, because the pQCT studies in former and continuing throwers preceded the QCT study in active throwers. A tomographic slice (thickness = 2.3 mm; voxel size = 300 μm; scan speed = 20 mm/s) was taken at 50% of humeral length (midshaft) from a reference line placed through the radiohumeral joint. Tomographic slices were analyzed for bone mineral density, structure, estimated strength, and muscle cross-sectional area. Cortical mode 1 (threshold, 710 mg/cm^3) was used to obtain cortical volumetric bone mineral density (mg/cm^3), bone mineral content (mg/mm), and area (cm^2). Total area (cm^2), trabecular/subcortical bone mineral content (mg/mm), and average cortical thickness (mm) were obtained by analyzing the slices using contour mode 1 (threshold, 710 mg/cm^3) to define the outer bone edge and peel mode 2 (threshold, 400 mg/cm^3) to separate the cortical and subcortical/trabecular bone compartments. Cortical thickness measurements used a circular ring model, and medullary area (mm^2) was derived as total area minus cortical area. Bone strength was estimated by the derivation of density-weighted polar moment of inertia (cm^4). The muscle cross-sectional area (cm^2) was assessed by using contour mode 3 (threshold, −100 mg/cm^3) to locate the skin surface and peel mode 2 (threshold, 40 mg/cm^3) to locate the subcutaneous fat–muscle boundary. A 3 × 3 kernel filter to filter all voxels between −500 and 500 mg/cm^3 followed by a 5 × 5 kernel filter to filter all voxels between −500 and 300 mg/cm^3 (F03F05 filter) was used to remove noise.

Statistical Analyses. Analyses were performed with IBM SPSS Statistics (v20.0; SPSS Inc.) and were two-tailed with a level of significance set at 0.05. Demographic and anthropometric characteristics were compared between groups using independent-sample *t* tests (active throwers vs. controls and former throwers vs. controls) or one-way ANOVA followed by Tukey pairwise comparisons (continuing throwers vs. former throwers vs. controls). Side-to-side differences between the throwing and nonthrowing arms in throwers were assessed by calculating absolute (throwing − nonthrowing) and mean percent differences [(throwing − nonthrowing)/nonthrowing × 100] and their 95% confidence intervals (CI). A 95% CI not crossing zero was considered statistically significant, as determined by single-sample *t* tests with a population mean of 0%. Similar analyses were performed to determine side-to-side differences between the dominant and nondominant arms in controls. Throwing effects on the arm were determined by comparing the absolute or percent difference values between activity groups (throwers vs. controls) using independent-sample *t* tests (active throwers vs. controls and former throwers vs. controls) or one-way ANOVA followed by Tukey pairwise comparisons (continuing throwers vs. former throwers vs. controls).

1. Warden SJ, Bogenschutz ED, Smith HD, Gutierrez AR (2009) Throwing induces substantial torsional adaptation within the midshaft humerus of male baseball players. *Bone* 45(5):931–941.
2. Garner BA, Pandy MG (2001) Musculoskeletal model of the upper limb based on the visible human male dataset. *Comput Methods Biomech Biomed Engin* 4(2):93–126.
3. Garner BA, Pandy MG (2003) Estimation of musculotendon properties in the human upper limb. *Ann Biomed Eng* 31(2):207–220.
4. Garner BA, Pandy MG (2000) The obstacle-set method for representing muscle paths in musculoskeletal models. *Comput Methods Biomech Biomed Engin* 3(1):1–30.
5. Fleisig GS, Bolt B, Fortenbaugh D, Wilk KE, Andrews JR (2011) Biomechanical comparison of baseball pitching and long-toss: implications for training and rehabilitation. *J Orthop Sports Phys Ther* 41(5):296–303.
6. Yanagawa T, et al. (2008) Contributions of the individual muscles of the shoulder to glenohumeral joint stability during abduction. *J Biomech Eng* 130(2):021024.
7. Rho JY, Hobatho MC, Ashman RB (1995) Relations of mechanical properties to density and CT numbers in human bone. *Med Eng Phys* 17(5):347–355.

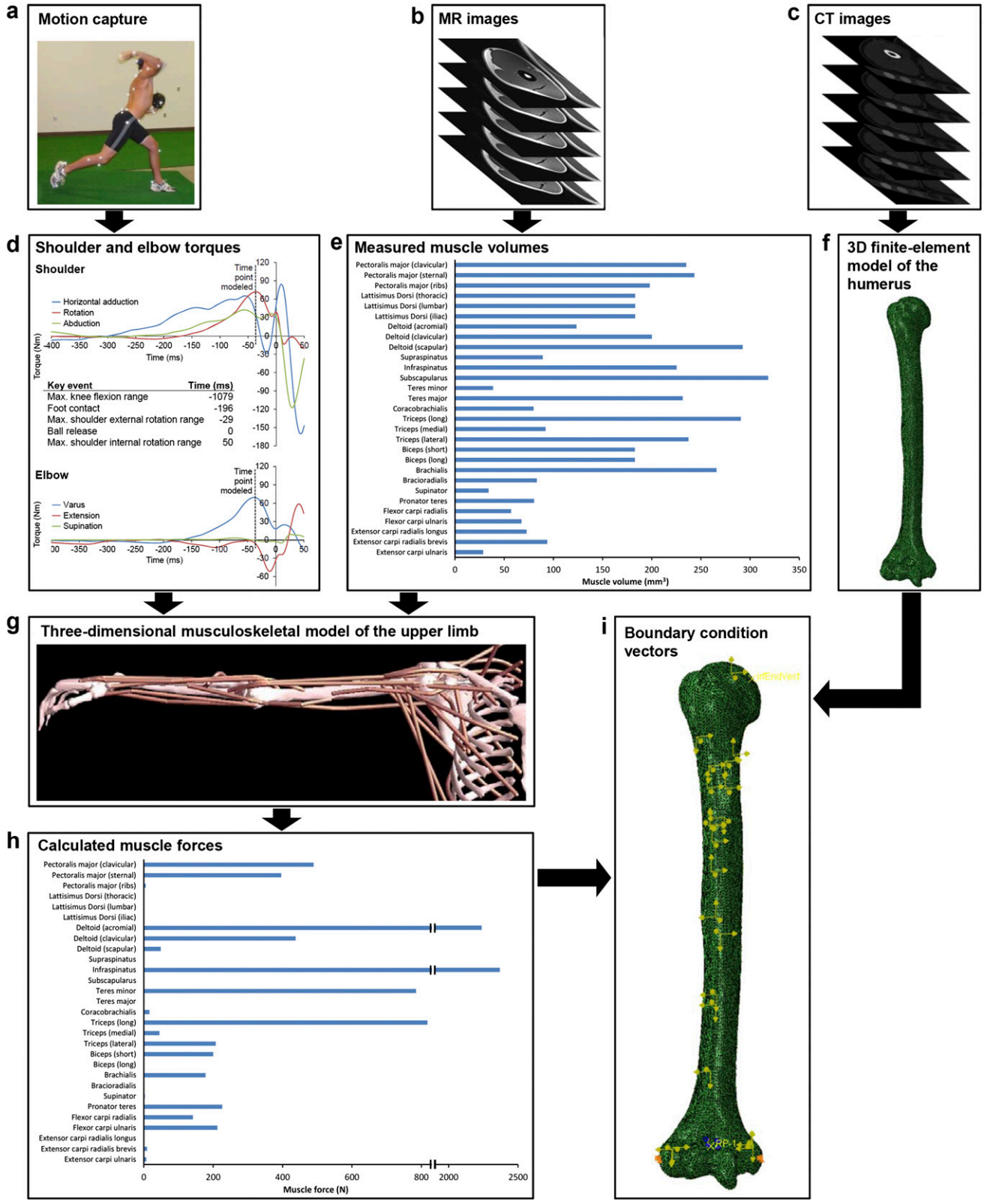

Fig. S1. Subject-specific musculoskeletal model of the upper extremity and CT-based finite-element model of the humerus during pitching. (*A* and *D*) An MLB pitcher threw fastball pitches in an indoor biomechanics laboratory (*A*) to obtain 3D torques and joint angles at the shoulder and elbow (*D*). Peak shoulder axial rotation and elbow varus torques were coincident and occurred toward the late cocking phase of the pitching motion (near maximum shoulder external rotation range, which occurred 29 ms before ball release). Torques and joint angles during this phase of the pitching motion were used in the musculoskeletal model. (*B* and *E*) MR images of the player's upper extremity (*B*) were obtained to determine muscle volumes (*E*). (*G* and *H*) The subject-specific torques, angles, and muscle volumes were introduced to the 3D musculoskeletal model of the upper limb developed by Garner and Pandy (2) (*G*) to calculate musculoskeletal

Legend continued on following page

forces (muscle and joint reaction forces) (*H*). (*C* and *F*) High-resolution CT images of the player's upper extremity (*C*) were obtained and converted into an FE model (*F*). (*I*) The muscle and joint reaction forces from the musculoskeletal model were applied to the FE model to calculate tensile and shear strains.

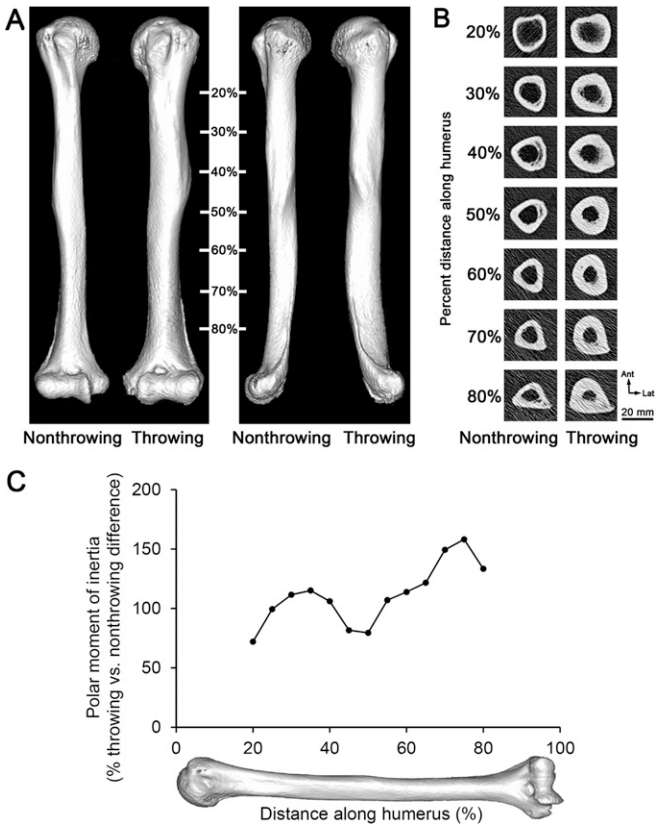

Fig. S2. CT images and strength measures of the humerii in the MLB/MiLB player demonstrating the greatest difference between the throwing arm and the nonthrowing arm. (*A*) In the reconstructed images, notice the more robust diaphysis with visibly broader diameter on the throwing side when viewed anteriorly (*Left*) and laterally (*Right*). (*B*) Cross-sectional images of the humerii in *A* at increments of 10% of humeral length revealed substantially greater total and cortical bone areas and cortical thickness and smaller medullary area in the throwing arm at each increment. (*C*) Percent difference in torsional bone strength in the throwing arm vs. the nonthrowing arm (indicated by density-weighted polar moment of inertia) at 5% increments along the diaphysis for the humerii shown in *A* and *B*. The throwing arm was more than twice as strong, on average, as the contralateral nonthrowing arm and was more than 2.5 times stronger in the distal diaphysis.

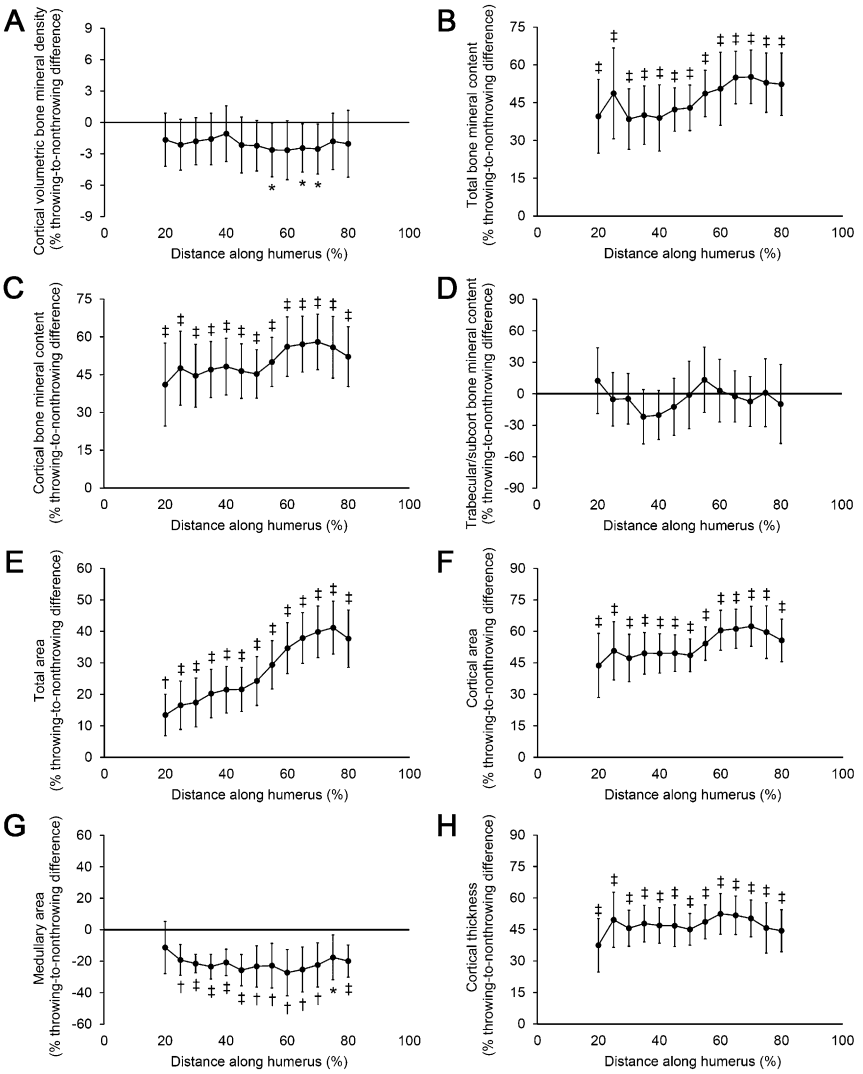

Fig. S3. Mean (± 95% CI) percent difference between the throwing arm and the nonthrowing arm at 5% increments of humeral length in active throwers normalized to the differences between the dominant arm and nondominant arm in controls in (*A*) cortical volumetric bone mineral density; (*B*) total bone mineral content; (*C*) cortical bone mineral content; (*D*) trabecular/subcortical bone mineral content; (*E*) total cross-sectional area; (*F*) cortical cross-sectional area; (*G*) medullary cross-sectional area; and (*H*) cortical thickness. CIs greater or less than 0% indicate differences between the throwing arm and the nonthrowing arm in active throwers that are greater or less, respectively, than the differences between the dominant arm and the nondominant arm in controls (*$P < 0.05$; $^{\dagger}P < 0.01$; $^{\ddagger}P < 0.001$, unpaired *t* test). Throwing had a minimal effect on cortical volumetric bone mineral density, had no effect on trabecular/subcortical bone mineral content, reduced the medullary area, and increased the total and cortical bone mineral content, total area, cortical area, and cortical thickness.

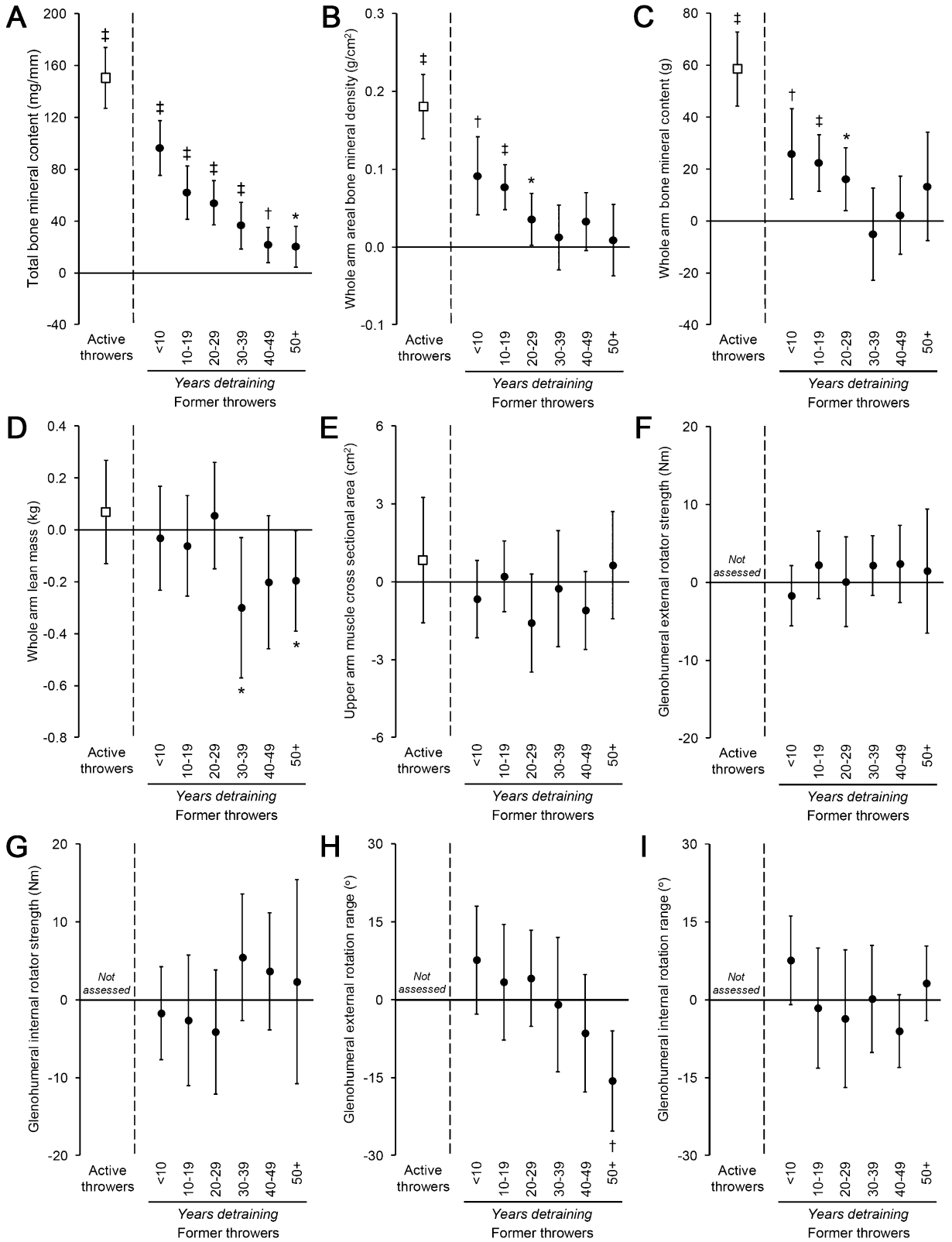

Fig. S4. Mean (± 95% CI) differences between the throwing arm and the nonthrowing arm in former throwers normalized to the differences between the dominant arm and the nondominant arm in controls for (*A*) pQCT-derived total bone mineral content at the midshaft humerus; (*B*) DXA-derived whole-arm areal bone mineral density; (*C*) DXA-derived whole arm bone mineral content; (*D*) DXA-derived whole arm lean mass; (*E*) pQCT-derived upper arm muscle cross-sectional area; (*F*) glenohumeral external rotator strength; (*G*) glenohumeral internal rotator strength; (*H*) glenohumeral external rotation range; and (*I*) glenohumeral internal rotation range. CIs greater or less than 0% indicate differences between the throwing arm and the nonthrowing arm in former throwers that are greater or less, respectively, than the differences between the dominant arm and the nondominant arm in controls (*$P < 0.05$; †$P < 0.01$; ‡$P <$

Legend continued on following page

0.001, unpaired *t* test). The benefit of throwing on areal bone mineral density and content were no longer present after 30–39 y detraining. The difference in the whole-arm lean mass between the throwing arm and the nonthrowing arm was smaller in former throwers in the 30–39 and 50+ detraining groups than in controls. The difference in the glenohumeral external rotation range between the throwing arm and the nonthrowing arm was smaller in former throwers in the 50+ detraining group than in controls.

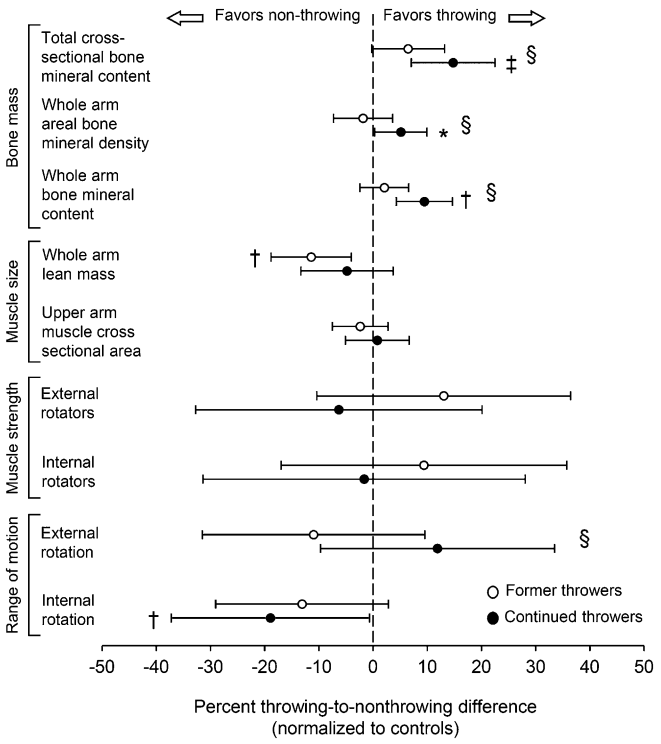

Fig. S5. Mean (± 95% CI) percent differences between the throwing arm and the nonthrowing arm in former and continuing throwers relative to the differences between the dominant and nondominant arm in controls for pQCT-derived total bone mineral content and upper arm muscle cross sectional area; DXA-derived whole arm areal bone mineral density; bone mineral content; whole-arm lean mass; and glenohumeral external and internal rotator strength and rotation range. CIs greater or less than 0% indicate differences between the throwing arm and the nonthrowing arm in throwers that are greater or less, respectively, than the differences between the dominant arm and the nondominant arm in controls (*$P < 0.05$; †$P < 0.01$). § indicates a significant difference between former and continuing throwers ($P < 0.05$). Continuing throwers had (*i*) greater percent differences in total bone mineral content and whole-arm areal bone mineral density and bone mineral content than either former throwers or controls; (*ii*) greater percent differences in the external rotation range than former throwers; and (*iii*) smaller percent differences in the internal rotation range than controls. Former throwers had smaller percent differences for whole-arm lean mass than controls. Statistics were performed with one-way ANOVA followed by Tukey pairwise comparisons (continuing throwers vs. former throwers vs. controls).

Table S1. Demographic and anthropometric characteristics of active throwers and controls

Characteristic	Controls	Active throwers
Subjects, *n*	8	9
Demographics		
Age, y	27.1 ± 3.8	27.9 ± 2.2
Estimated age of adolescent growth spurt, y	13.0 ± 0.9	13.8 ± 1.3
Age started throwing, y	–	6.3 ± 2.8
Years throwing before adolescent growth spurt	–	7.5 ± 2.9
Playing position during professional career (pitcher/catcher)	–	9/0
Professional (MLB/MiLB) games played, *n*	–	220 ± 84
Professional (MLB/MiLB) innings pitched, *n*	–	693 ± 326
Total years throwing	–	21.2 ± 2.5
Whole-body anthropometry		
Height, m	1.91 ± 0.07	1.87 ± 0.08
Mass, kg	102.1 ± 11.2	92.2 ± 17.9
Body mass index, kg/m^2	26.2 ± 4.6	27.9 ± 2.9
Areal bone mineral density, g/cm^{2†,‡}	1.28 ± 0.17	1.29 ± 0.09
Lean mass, kg‡	62.5 ± 10.3	74.5 ± 6.9*
Fat mass, %‡	25.3 ± 7.5	20.9 ± 3.8
Regional anthropometry		
Spine areal bone mineral density, g/cm^{2†,‡}	1.22 ± 0.17	1.14 ± 0.07
Hip areal bone mineral density, g/cm^{2†,‡}	1.19 ± 0.10	1.23 ± 0.11

Data are mean ± SD, except for frequencies. MLB/MiLB, Major/Minor League Baseball.
*$P < 0.05$ vs. controls, as determined by unpaired *t* test.
†Values corrected for whole-body lean mass.
‡Obtained via dual-energy X-ray absorptiometry.

Table S2. Demographic and anthropometric characteristics of former throwers and controls

	Years detraining											
	<10		10–19		20–29		30–39		40–49		50+	
Characteristic	Controls	Former throwers	Controls	Former throwers	Controls	Former throwers	Controls	Former throwers	Controls	Former throwers	Controls	Former throwers
Subjects, *n*	19	18	14	22	18	16	10	12	14	9	11	7
Demographics												
Age, y	34.6 ± 3.1	37.1 ± 4.6	45.2 ± 3.3	44.9 ± 4.0	54.5 ± 3.1	55.9 ± 5.4	65.1 ± 3.5	65.3 ± 5.4	75.2 ± 2.9	72.8 ± 2.8	83.8 ± 2.5	83.8 ± 2.3
Estimated age of adolescent growth spurt, y	13.2 ± 1.4	13.9 ± 1.2	13.8 ± 1.0	14.2 ± 1.3	13.9 ± 1.1	14.4 ± 1.5	13.0 ± 1.6	13.5 ± 1.2	14.6 ± 1.6	14.0 ± 1.6	14.5 ± 1.4	14.6 ± 0.5
Age started throwing, y	–	5.8 ± 1.9	–	6.0 ± 1.5	–	7.4 ± 2.0	–	6.7 ± 1.9	–	6.3 ± 2.5	–	5.4 ± 0.5
Years throwing before adolescent growth spurt	–	8.1 ± 2.1	–	8.2 ± 2.5	–	7.0 ± 2.7	–	6.8 ± 2.4	–	7.8 ± 1.9	–	9.0 ± 0.7
Playing position during professional career (pitcher/catcher)	–	17/1	–	20/2	–	12/4	–	12/0	–	8/1	–	7/0
Professional (MLB/MiLB) games played, *n*	–	414 ± 301	–	326 ± 138	–	507 ± 363	–	345 ± 217	–	444 ± 235	–	418 ± 126
Professional (MLB/MiLB) innings pitched, *n*[†]	–	959 ± 495	–	888 ± 366	–	1518 ± 1110	–	1233 ± 450	–	1246 ± 474	–	1964 ± 789*,**
Age ceased throwing, y	–	31.6 ± 3.6	–	31.3 ± 3.1	–	31.4 ± 4.8	–	31.5 ± 5.0	–	31.0 ± 3.1	–	31.2 ± 1.8
Total years throwing	–	25.7 ± 3.4	–	25.3 ± 3.3	–	24.0 ± 4.6	–	24.8 ± 5.3	–	25.8 ± 1.3	–	24.2 ± 4.5
Total years detraining	–	5.5 ± 2.0***	–	13.6 ± 3.2***	–	24.6 ± 2.8***	–	33.8 ± 2.4***	–	42.4 ± 3.7***	–	52.6 ± 2.2***
Whole-body anthropometry												
Height, m	1.76 ± 0.06	1.89 ± 0.08****	1.81 ± 0.10	1.88 ± 0.05****	1.76 ± 0.05	1.87 ± 0.07****	1.74 ± 0.08	1.85 ± 0.07****	1.74 ± 0.09	1.79 ± 0.08	1.74 ± 0.06	1.82 ± 0.07****
Mass, kg	80.0 ± 14.6	102.3 ± 10.6****	92.2 ± 21.1	104.8 ± 18.2	84.4 ± 18.4	111.7 ± 12.4****	91.8 ± 20.2	110.9 ± 19.4****	83.9 ± 13.9	95.2 ± 13.0	81.8 ± 13.8	92.7 ± 7.2
Body mass index, kg/m^2	25.9 ± 4.4	28.8 ± 3.3*	28.0 ± 5.4	29.7 ± 4.7	27.0 ± 4.6	32.2 ± 4.4****	30.0 ± 6.4	32.0 ± 4.9	27.7 ± 2.6	29.9 ± 4.2	27.0 ± 4.1	28.0 ± 2.0
Areal bone mineral density, g/cm^{2‡,§}	1.30 ± 0.09	1.33 ± 0.12	1.30 ± 0.12	1.38 ± 0.10****	1.30 ± 0.12	1.47 ± 0.17****	1.35 ± 0.15	1.35 ± 0.10	1.26 ± 0.16	1.41 ± 0.17	1.27 ± 0.15	1.28 ± 0.10
Lean mass, kg[§]	53.2 ± 6.8	70.8 ± 6.5****	60.8 ± 12.1	64.4 ± 15.5	56.4 ± 9.7	69.4 ± 9.3****	54.0 ± 10.2	69.2 ± 9.9****	50.8 ± 8.2	58.2 ± 2.8	48.5 ± 6.7	56.9 ± 7.3****
Fat mass, %[‡,§]	27.7 ± 7.1	25.9 ± 3.8	28.4 ± 4.6	28.2 ± 4.3	27.9 ± 6.0	31.4 ± 4.2	35.8 ± 7.1	32.9 ± 4.9	33.5 ± 5.5	30.3 ± 4.8	34.2 ± 4.9	32.3 ± 2.0
Regional anthropometry												
Spine areal bone mineral density, g/cm^{2‡,§}	1.07 ± 0.09	1.10 ± 0.10	1.09 ± 0.16	1.13 ± 0.13	1.08 ± 0.19	1.24 ± 0.21	1.18 ± 0.13	1.21 ± 0.13	1.13 ± 0.19	1.23 ± 0.08	1.17 ± 0.23	1.20 ± 0.13
Hip areal bone mineral density, g/cm^{2‡,§}	1.05 ± 0.12	1.08 ± 0.11	1.00 ± 0.11	1.07 ± 0.11	1.00 ± 0.11	1.14 ± 0.17*	1.07 ± 0.15	1.12 ± 0.10	0.90 ± 0.12	1.05 ± 0.12*	0.93 ± 0.08	0.98 ± 0.11

Data are mean ± SD, except for frequencies. MLB/MiLB, Major/Minor League Baseball. Significance is indicated by asterisks: *$P < 0.05$ vs. former throwers who ceased playing 10–19 y ago; **$P < 0.05$ vs. former throwers who ceased playing 20–29 y ago; ***$P < 0.05$ vs. all other years detraining groups, all determined by one-way ANOVA followed by Bonferroni pairwise comparisons; ****$P < 0.05$ vs. controls in the same years detraining cohort, as determined by unpaired *t* test.

[†]Data only for subjects who played as a pitcher.

[‡]Values corrected for whole-body lean mass.

[§]Obtained via dual-energy X-ray absorptiometry.

Table S3. Midshaft humerus properties in former throwers and controls

		Controls				Former throwers			
Bone measure	Years detraining	Nondominant†	Dominant†	Absolute difference (95% CI)‡	% difference (95% CI)‡	Nonthrowing†	Throwing†	Absolute difference (95% CI)‡	% difference (95% CI)‡
Cortical volumetric bone mineral density, mg/cm^3	0 (active throwers)	1,186 ± 17	1,189 ± 12	3 (−7, 13)	0.3 (−0.6, 1.1)	1,162 ± 18	1,152 ± 17	−10 (−20, −1)*	−0.9 (−1.7, −0.1)*
	<10	1,171 ± 19	1,166 ± 21	−5 (−9, −1)*	−0.4 (−0.8, −0.1)*	1,150 ± 29	1,141 ± 27	−9 (−16, 11)	−0.8 (−1.5, −0.1)*
	10–19	1,157 ± 31	1,149 ± 32	−8 (−12, −4)**	−0.7 (−1.0, −0.4)*	1,153 ± 24	1,138 ± 28	−15 (−20, −9)***	−1.3 (−1.8, −0.8)***
	20–29	1,145 ± 38	1,135 ± 37	−9 (−13, −5)***	−0.8 (−1.2, −0.4)***	1,133 ± 41	1,117 ± 41	−16 (−22, −9)***	−1.4 (−2.0, −0.8)***
	30–39	1,133 ± 36	1,128 ± 38	−5 (−14, 4)	−0.4 (−1.2, 0.4)	1,128 ± 35	1,117 ± 33	−11 (−23, 1)	−0.9 (−2.0, 0.1)
	40–49	1,144 ± 26	1,133 ± 26	−11 (−22, −1)*	−1.0 (−1.9, 0.1)	1,147 ± 29	1,134 ± 19	−13 (−25, −1)***	−1.1 (−2.1, −0.1)*
	50+	1,122 ± 40	1,109 ± 36	−13 (−26, 1)	−1.1 (−2.3, 0.1)	1,090 ± 41	1,083 ± 31	−8 (−34, 18)	−0.7 (−3.1, 1.8)
Total bone mineral content, mg/mm	0 (active throwers)	361.3 ± 76.4	370.6 ± 67.2	9.3 (-6.0, 24.7)	3.1 (−1.0, 7.2)	339.0 ± 33.3	498.9 ± 48.9	159.9 (139.5, 180.2)***	47.3 (41.5, 53.1)***
	<10	300.3 ± 38.3	311.8 ± 40.0	11.6 (5.4, 17.7)**	3.9 (1.9, 6.0)**	334.2 ± 31.5	442.0 ± 57.7	107.8 (85.8, 129.7)***	32.3 (25.8, 38.9)***
	10–19	323.3 ± 43.2	335.7 ± 46.0	12.4 (5.9, 18.9)**	3.9 (1.7, 6.0)**	347.6 ± 33.7	421.4 ± 52.9	73.8 (57.5, 90.2)***	21.3 (16.9, 25.8)***
	20–29	312.9 ± 47.1	323.1 ± 51.6	10.2 (4.5, 15.8)**	3.2 (1.3, 5.0)**	342.6 ± 33.8	406.3 ± 55.4	63.7 (45.4, 82.0)***	18.5 (13.5, 23.5)***
	30–39	282.5 ± 17.3	299.0 ± 20.7	16.5 (4.5, 28.4)*	6.0 (1.7, 10.2)*	328.8 ± 41.0	381.1 ± 58.3	52.3 (37.7, 67.0)***	15.6 (11.9, 19.3)***
	40–49	286.0 ± 45.4	294.1 ± 48.1	8.1 (2.0, 14.2)*	2.8 (0.9, 4.8)**	341.1 ± 19.8	370.2 ± 23.2	29.1 (11.7, 46.5)**	8.7 (3.3, 114.0)**
	50+	265.5 ± 36.6	275.2 ± 45.7	9.7 (0.5, 18.9)	3.3 (−0.2, 6.8)	316.8 ± 30.0	346.0 ± 36.9	29.2 (11.8, 46.6)*	9.2 (3.8, 14.6)**
Cortical bone mineral content, mg/mm	0 (active throwers)	347.5 ± 77.0	357.3 ± 68.4	9.8 (−6.3, 26.0)	3.4 (−1.0, 7.7)	319.5 ± 31.9	479.6 ± 45.5	160.2 (141.2, 179.2)***	50.4 (44.2, 56.6)***
	<10	289.3 ± 37.3	300.3 ± 39.2	11.0 (4.5, 17.5)**	3.9 (1.6, 6.2)**	316.7 ± 35.4	417.7 ± 64.5	101.0 (77.2, 124.7)***	31.9 (24.4, 39.5)***
	10–19	307.3 ± 41.3	317.6 ± 45.3	10.3 (2.7, 17.9)**	3.3 (0.8, 5.9)*	331.0 ± 31.1	393.3 ± 51.8	62.3 (44.9, 79.6)***	18.9 (13.9, 23.9)***
	20–29	295.3 ± 48.4	302.1 ± 52.0	6.8 (1.2, 12.4)*	2.2 (0.2, 4.2)*	321.7 ± 38.5	370.1 ± 64.3	48.4 (28.6, 68.2)***	14.6 (9.0, 20.3)***
	30–39	260.6 ± 25.7	272.5 ± 18.8	11.9 (−1.1, 25.0)	5.1 (−0.3, 10.4)	303.3 ± 44.3	341.0 ± 62.2	37.8 (21.6, 53.9)***	12.0 (7.3, 16.7)***
	40–49	267.3 ± 49.7	271.5 ± 53.0	4.2 (−2.5, 10.9)	1.5 (−0.9, 3.9)	323.6 ± 23.0	337.5 ± 28.9	13.9 (−7.2, 35.0)	4.5 (−2.4, 11.3)
	50+	237.1 ± 46.8	240.6 ± 53.9	3.5 (−5.7, 12.6)	1.0 (−3.6, 5.2)	282.6 ± 29.6	292.5 ± 28.3	9.9 (−6.7, 26.5)	3.6 (−2.1, 9.4)
Trabecular/ subcortical bone mineral content, mg/mm	0 (active throwers)	6.28 ± 3.20	6.77 ± 2.75	0.48 (−0.67, 1.64)	12.9 (−6.7, 32.5)	8.89 ± 3.56	8.11 ± 3.00	−0.77 (−2.27, 0.72)	−5.3 (−25.6, 14.9)
	<10	5.48 ± 2.66	5.76 ± 2.29	0.29 (−0.15, 0.73)	9.2 (0.2, 18.3)*	7.62 ± 2.63	10.60 ± 3.38	2.98 (2.07, 3.90)***	42.2 (27.7, 56.7)***
	10–19	7.26 ± 3.08	8.26 ± 4.20	1.00 (−0.01, 2.01)	10.8 (−2.9, 24.5)	7.08 ± 2.32	11.55 ± 3.85	4.48 (3.19, 5.76)***	67.0 (49.0, 85.0)***
	20–29	7.98 ± 2.90	9.31 ± 3.06	1.32 (0.32, 2.33)*	20.0 (5.5, 34.6)*	9.24 ± 4.46	15.10 ± 4.26	5.86 (4.02, 7.69)***	83.2 (46.4, 119.9)***
	30–39	10.14 ± 8.36	10.63 ± 5.52	0.49 (−2.95, 3.93)	22.0 (−4.8, 48.7)	11.13 ± 5.54	18.36 ± 6.73	7.23 (5.84, 8.63)***	76.3 (50.7, 101.9)***
	40–49	8.67 ± 4.79	10.38 ± 5.37	1.71 (0.72, 2.70)**	24.8 (12.2, 37.3)**	8.16 ± 3.37	16.03 ± 6.29	7.87 (4.24, 11.50)***	104.5 (61.8, 147.2)**
	50+	12.60 ± 8.56	15.55 ± 9.93	2.95 (0.85, 5.05)*	28.2 (9.1, 47.4)**	14.51 ± 5.84	26.66 ± 9.56	12.14 (5.06, 19.22)***	93.0 (34.7, 151.3)***
Total area, cm^2	0 (active throwers)	3.91 ± 0.60	4.03 ± 0.54	0.12 (−0.02, 0.25)	3.3 (−0.4, 7.0)	4.39 ± 0.60	5.53 ± 0.72	1.13 (0.88, 1.38)***	26.0 (19.8, 32.2)***
	<10	3.45 ± 0.45	3.64 ± 0.46	0.19 (0.13, 0.24)***	5.5 (3.7, 7.2)***	4.22 ± 0.40	5.31 ± 0.31	1.09 (0.96, 1.22)***	26.6 (22.4, 30.7)***
	10–19	3.90 ± 0.54	4.18 ± 0.66	0.28 (0.17, 0.40)***	7.1 (4.5, 9.8)***	4.30 ± 0.44	5.31 ± 0.46	1.01 (0.92, 1.10)***	23.9 (21.5, 26.2)***
	20–29	3.93 ± 0.48	4.20 ± 0.56	0.27 (0.21, 0.33)‡	6.8 (5.4, 8.3)***	4.50 ± 0.58	5.57 ± 0.55	1.07 (0.89, 1.25)***	24.4 (19.8, 29.1)***
	30–39	3.74 ± 0.80	4.03 ± 0.78	0.29 (0.10, 0.48)**	8.4 (3.3, 13.4)**	4.53 ± 0.70	5.67 ± 0.68	1.13 (1.02, 1.25)***	25.7 (21.5, 29.9)***
	40–49	3.79 ± 0.49	4.12 ± 0.50	0.33 (0.25, 0.41)***	9.0 (6.7, 11.2)***	4.31 ± 0.33	5.27 ± 0.42	0.96 (0.85, 1.07)***	22.2 (20.3, 24.2)***
	50+	3.96 ± 0.85	4.37 ± 0.92	0.41 (0.29, 0.53)***	10.5 (8.0, 13.0)***	4.65 ± 0.49	5.62 ± 0.56	0.98 (0.69, 1.26)**	21.2 (14.7, 27.6)***

Table S3. Cont.

Bone measure	Years detraining	Controls				Former throwers			
		Nondominant†	Dominant†	Absolute difference (95% CI)‡	% difference (95% CI)‡	Nonthrowing†	Throwing†	Absolute difference (95% CI)‡	% difference (95% CI)‡
Cortical area, cm^2	0 (active throwers)	2.93 ± 0.64	3.00 ± 0.56	0.07 (−0.06, 0.21)	3.1 (−1.2, 7.5)	2.75 ± 0.27	4.17 ± 0.39	1.42 (1.26, 1.57)***	51.7% (45.9, 57.4)***
	<10	2.47 ± 0.33	2.58 ± 0.35	0.11 (0.05, 0.17)**	4.4 (1.9, 6.9)**	2.75 ± 0.29	3.66 ± 0.52	0.90 (0.70, 1.10)***	33.0 (25.5, 40.5)***
	10–19	2.66 ± 0.37	2.77 ± 0.40	0.11 (0.04, 0.18)**	4.1 (1.5, 6.6)**	2.87 ± 0.27	3.46 ± 0.44	0.58 (0.44, 0.73)***	20.4 (15.6, 25.1***
	20–29	2.58 ± 0.39	2.66 ± 0.42	0.08 (0.03, 0.13)*	3.0 (1.0, 5.0)**	2.82 ± 0.27	3.30 ± 0.49	0.47 (0.31, 0.64)***	16.4 (11.0, 21.9)***
	30–39	2.30 ± 0.19	2.42 ± 0.14	0.12 (0.58, 22.8)*	5.5 (0.4, 10.5)*	2.69 ± 0.39	3.05 ± 0.54	0.36 (0.23, 0.49)***	13.0 (8.7, 17.3)***
	40–49	2.33 ± 0.41	2.39 ± 0.44	0.06 (−0.01, 0.13)	2.5% (−0.3, 5.4%)	2.82 ± 0.21	2.98 ± 0.27	0.15 (−0.04, 0.35)	5.6 (−1.5, 12.8)
	50+	2.10 ± 0.37	2.16 ± 0.45	0.06 (−0.02, 0.14)	2.4 (−1.5, 6.2)	2.59 ± 0.26	2.71 ± 0.30	0.11 (−0.05, 0.28)	4.4 (−1.8, 10.6)
Medullary area, cm^2	0 (active throwers)	0.98 ± 0.41	1.02 ± 0.39	0.04 (−0.04, 0.12)	5.8 (−2.7, 14.2)	1.64 ± 0.46	1.36 ± 0.43	−0.28 (−0.45, −0.12)**	−17.1 (−29.2, −5.0)*
	<10	0.98 ± 0.27	1.06 ± 0.27	0.08 (0.04, 0.12)***	9.0 (5.5, 12.5)***	1.46 ± 0.44	1.65 ± 0.53	0.19 (0.04, 0.34)*	13.9 (5.2, 22.7)**
	10–19	1.24 ± 0.35	1.42 ± 0.51	0.18 (0.04, 0.18)*	12.4 (2.6, 22.2)*	1.42 ± 0.30	1.86 ± 0.39	0.43 (0.30, 0.56)***	32.8 (21.0, 44.7)**
	20–29	1.35 ± 0.33	1.54 ± 0.39	0.19 (0.13, 0.25)***	14.3 (9.9, 18.7)***	1.67 ± 0.62	2.27 ± 0.74	0.47 (0.31, 0.64)***	39.6 (24.7, 54.5)***
	30–39	1.44 ± 0.87	1.62 ± 0.78	0.18 (−0.02, 0.37)	18.6 (4.7, 10.5)*	1.84 ± 0.64	2.61 ± 0.64	0.77 (0.64, 0.90)***	48.6 (31.9, 65.4)***
	40–49	1.45 ± 0.57	1.73 ± 0.66	0.27 (0.18, 0.37)***	19.9 (13.1, 26.8)***	1.49 ± 0.39	2.29 ± 0.56	0.81 (0.53, 1.08)***	57.4 (36.8, 78.0)***
	50+	1.85 ± 0.99	2.21 ± 1.08	0.35 (0.21, 0.49)***	20.0 (13.8, 26.1)***	2.06 ± 0.41	2.92 ± 0.49	0.86 (0.57, 1.16)***	43.2 (27.5, 58.9)**
Cortical thickness, mm	0 (active throwers)	5.64 ± 1.27	5.68 ± 1.13	0.04 (−0.22, 0.30)	1.2 (−2.9, 5.4)	4.63 ± 0.46	6.74 ± 0.51	2.10 (1.86, 2.35)***	45.9 (39.1, 52.7)***
	<10	4.93 ± 0.59	4.98 ± 0.58	0.05 (−0.05, 0.16)	1.1 (−1.2, 3.5)	4.82 ± 0.69	5.83 ± 1.08	1.00 (0.66, 1.35)***	20.9 (13.2, 28.5)***
	10–19	4.89 ± 0.57	4.89 ± 0.73	0.01 (−0.19, 0.20)	−0.1 (−4.0, 3.9)	4.99 ± 0.45	5.35 ± 0.73	0.36 (0.08, 0.64)*	7.4 (1.9, 12.9)**
	20–29	4.66 ± 0.69	4.59 ± 0.69	−0.07 (−0.17, 0.02)	1.5 (−3.7, 0.7)	4.75 ± 0.71	4.90 ± 1.01	0.15 (−0.17, 0.46)	2.8 (−3.6, 9.3)
	30–39	4.34 ± 0.86	4.30 ± 0.70	−0.04 (−0.27, 0.19)	0.2 (−6.2, 6.6)	4.44 ± 0.81	4.35 ± 0.86	−0.08 (−0.29, 0.13)	−2.0 (−6.6, 2.6)
	40–49	4.27 ± 0.94	4.14 ± 0.99	−0.14 (−0.26, −0.01)*	−3.4 (−6.5, −0.3)*	4.88 ± 0.63	4.46 ± 0.63	−0.43 (−0.83–0.02)*	−8.5 (−17.0, 0.1)
	50+	3.69 ± 0.90	3.56 ± 1.00	−0.13 (−0.28, 0.02)	−4.1 (−8.1, −0.2)*	4.10 ± 0.45	3.76 ± 0.46	−0.34 (−0.56, −0.12)*	−8.3 (−13.3, −3.3)**
Polar moment of inertia, cm^4	0 (active throwers)	2.45 ± 0.76	2.59 ± 0.71	0.13 (−0.04, 0.31)	6.7 (−0.9, 14.2)	2.79 ± 0.62	4.75 ± 1.09	1.96 (1.49, 2.43)***	70.7 (56.1, 85.3)***
	<10	1.87 ± 0.44	2.05 ± 0.48	0.19 (0.12, 0.25)***	10.4 (6.7, 14.2)***	2.61 ± 0.41	4.17 ± 0.53	1.56 (1.35, 1.78)***	62.0 (51.3, 72.8)***
	10–19	2.32 ± 0.59	2.62 ± 0.73	0.29 (0.17, 0.42)***	12.3 (7.9, 16.7)***	2.77 ± 0.54	4.09 ± 0.75	1.32 (1.15, 1.50)***	49.0 (42.9, 55.0)***
	20–29	2.30 ± 0.58	2.57 ± 0.71	0.28 (0.20, 0.36)***	11.6 (8.7, 14.6)***	2.89 ± 0.53	4.21 ± 0.63	1.32 (1.09, 1.55)***	47.3 (37.8, 56.8)***
	30–39	1.98 ± 0.56	2.31 ± 0.65	0.34 (0.15, 0.52)**	17.7 (8.4, 27.1)**	2.86 ± 0.73	4.15 ± 0.96	1.29 (1.07, 1.52)***	46.6 (38.7, 54.6)***
	40–49	2.06 ± 0.49	2.33 ± 0.48	0.28 (0.20, 0.35)***	14.4 (10.0, 18.8)***	2.76 ± 0.34	3.76 ± 0.44	1.00 (0.88, 1.11)***	36.2 (33.1, 39.3)***
	50+	2.01 ± 0.54	2.34 ± 0.67	0.33 (0.18, 0.47)***	16.0 (10.4, 21.7)***	2.84 ± 0.50	3.78 ± 0.71	0.94 (0.55, 1.33)**	33.4 (20.6, 46.3)**

Significance is indicated by asterisks: *$P < 0.05$, **$P < 0.01$, ***$P < 0.001$.

†Data are mean ± SD.

‡Mean absolute and percent side-to-side differences (nondominant vs. dominant [controls] or nonthrowing vs. throwing [active throwers]) were assessed using single-sample *t* tests with a population mean of 0%.

Table S4. Demographic and anthropometric characteristics of continuing and former throwers and controls

Characteristic	Controls	Former throwers	Continuing throwers
Subjects, *n*	18	16	10
Demographics			
Age, y	73.7 ± 3.6	72.1 ± 3.7	71.2 ± 3.8
Estimated age of adolescent growth spurt, y	14.4 ± 1.4	13.6 ± 1.4	14.0 ± 0.8
Age started throwing, y	–	7.0 ± 2.5	6.9 ± 2.9
Years throwing before adolescent growth spurt	–	6.6 ± 2.6	7.7 ± 2.6
Playing position during professional career, pitcher/catcher	–	15/1	9/1
Professional (MLB/MiLB) games played, *n*	–	461 ± 228	500 ± 212
Professional (MLB/MiLB) innings pitched, *n*	–	1,504 ± 892	1,757 ± 988
Age ceased throwing at professional level, y	–	33.3 ± 5.0	34.3 ± 5.5
Age ceased throwing, y	–	33.3 ± 5.0	56.7 ± 8.8*
Years throwing postprofessional career, y	–	–	24.6 ± 4.4
Total years throwing	–	26.3 ± 5.4	49.8 ± 7.3*
Years detraining	–	38.8 ± 5.8	14.5 ± 9.0*
Whole-body anthropometry			
Height, m	1.75 ± 0.09	1.82 ± 0.08	1.86 ± 0.06
Mass, kg	85.6 ± 14.3	100.3 ± 14.3**	107.0 ± 14.1**
Body mass index, kg/m^2	27.7 ± 2.8	30.1 ± 3.6	30.8 ± 3.2**
Areal bone mineral density, g/cm^{2†,‡}	1.35 ± 0.14	1.34 ± 0.20	1.34 ± 0.19
Lean mass, kg‡	51.3 ± 7.9	62.6 ± 7.1**	66.8 ± 6.3**
Fat mass, %‡	34.2 ± 5.7	32.0 ± 4.2	32.1 ± 4.1
Regional anthropometry			
Spine areal bone mineral density, g/cm^{2†,‡}	1.24 ± 0.21	1.20 ± 0.16	1.23 ± 0.16
Hip areal bone mineral density, g/cm^{2†,‡}	0.99 ± 0.11	1.03 ± 0.11	1.03 ± 0.09

Data are mean ± SD, except for frequencies. MLB/MiLB, Major/Minor League Baseball. Significance is indicated by asterisks: *P < 0.001 vs. former throwers, as determined by unpaired t test; **P < 0.05 vs. controls, as determined via one-way ANOVA followed by Tukey post hoc comparisons.

†Values corrected for whole-body lean mass.

‡Obtained via dual-energy X-ray absorptiometry.